



Using the dual approach of FAO-56 for partitioning ET into soil and plant components for olive orchards in a semi-arid region

S. Er-Raki, Ghani Chehbouni, Gérard Boulet, D. G. Williams

► To cite this version:

S. Er-Raki, Ghani Chehbouni, Gérard Boulet, D. G. Williams. Using the dual approach of FAO-56 for partitioning ET into soil and plant components for olive orchards in a semi-arid region. *Agricultural Water Management*, 2010, 97 (11), pp.1769-1778. 10.1016/j.agwat.2010.06.009 . ird-00667360

HAL Id: ird-00667360

<https://hal.ird.fr/ird-00667360>

Submitted on 7 Feb 2012

HAL is a multi-disciplinary open access archive for the deposit and dissemination of scientific research documents, whether they are published or not. The documents may come from teaching and research institutions in France or abroad, or from public or private research centers.

L'archive ouverte pluridisciplinaire **HAL**, est destinée au dépôt et à la diffusion de documents scientifiques de niveau recherche, publiés ou non, émanant des établissements d'enseignement et de recherche français ou étrangers, des laboratoires publics ou privés.

**Using the dual approach of FAO-56 for partitioning ET into soil and plant
components for olive orchards in a semi-arid region**

S. Er-Raki^{1*}, A. Chehbouni², G. Boulet², D.G. Williams³

¹ Cadi Ayyad University / IRD, Marrakech, Morocco

Avenue Prince Moulay Abdellah, BP 2390 Marrakech 40000 (Morocco)

² Centre d'Etudes Spatiales de la Biosphère, Université de Toulouse, CNRS, IRD, CNES, 18

Avenue. Edouard Belin, bpi 2801, 31401 Toulouse cedex 9 (France)

³ Departments of Renewable Resources and Botany, University of Wyoming,

Laramie, WY 82071, USA

*Corresponding author and current address:

Dr. Salah Er-Raki

Projet SudMed - Centre Geber salle 26 –Faculty of Science Semlalia,

Cadi Ayyad University BP 2390, Marrakech, Morocco

Tel. /Fax. (+212) (0) 524 43 16 26

Email: s.erraki@ucam.ac.ma

Abstract

The main goal of this research was to evaluate the potential of the dual approach of FAO-56 for estimating actual crop evapotranspiration (AET) and its components (crop transpiration and soil evaporation) of an olive (*Olea europaea* L.) orchard in the semi arid region of Tensift-basin (central of Morocco). Two years (2003 and 2004) of continuous measurements of AET with the eddy covariance technique were used to test the performance of the model. The results showed that, by using the local values of basal crop coefficients, the approach simulates reasonably well AET over two growing seasons. The Root Mean Square Error (RMSE) between measured and simulated AET values during 2003 and 2004 were respectively about 0.54 and 0.71 mm per day. The obtained value of basal crop coefficient (K_{cb}) for the olive orchard was similar in both seasons with an average of 0.54. This value was lower than that suggested by the FAO-56 (0.62). Similarly, the single approach of FAO-56 has been tested in the previous work (Er-Raki et al., 2008) over the same study site and it has been shown that this approach also simulates correctly AET when using the local crop coefficient and under no stress conditions.

Since the dual approach predicts separately soil evaporation and plant transpiration, an attempt was made to compare the simulated components of AET with measurements obtained through a combination of eddy covariance and scaled-up sap flow measurements. The results showed that the model gives an acceptable estimate of plant transpiration and soil evaporation. The associated RMSE of plant transpiration and soil evaporation were 0.59 and 0.73 mm per day, respectively.

Additionally, the irrigation efficiency was investigated by comparing the irrigation scheduling design used by the farmer to those recommended by the FAO model. It was found that although the amount of irrigation applied by the farmer (800 mm) during the growing season of olives was twice that recommended one by the FAO model (411 mm), the

49 vegetation suffered from water stress during the summer. Such behaviour can be explained by
50 inadequate distribution of irrigation. Consequently, the FAO model can be considered as a
51 potentially useful tool for planning irrigation schedules on an operational basis.

52 **Keywords:** Crop coefficient, Evapotranspiration, Eddy covariance, FAO-56 model, Olea
53 europaea, Sap flow.

1. Introduction

Regions classified as semi-arid or arid constitute roughly one third of the total global land cover. Within these regions, water scarcity is one of the main factors limiting agricultural development. The impact of such water scarcity is amplified by inefficient irrigation practices, especially since the irrigation consumes more than 85% of the available water in these regions (Chehbouni et al., 2008). Therefore, the first step toward sound management of the scarce water resources in these regions requires an accurate estimation of the water needs and consumption of irrigated agriculture. The crop water need is defined as the amount of water needed to meet the **amount of** water lost to the atmosphere through evapotranspiration.

During the last two decades, several models have been developed to simulate crop evapotranspiration (ET) and in some cases, its components (soil evaporation and plant transpiration). These models ranged from complex, physically based ones such as the Simple Soil Plant Atmosphere SiSPAT (Braud et al., 1995), ISBA (Noilhan and Mahfouf, 1996), to more simple and conceptual ones (Sinclair and Seligman, 1996; Oliso et al., 1999) such as SVAT simple (Boulet et al., 2000). Other models such as STICS (Brisson, 1998) or CERRES (Ritchie, 1986) simulate ET through the combination of a water balance with a **crop** growth component. All of these models need several input parameters which cannot easily be obtained at the appropriate space-time scale, **and therefore difficult for operational applications.**

In addition to the above models/methods, the FAO-56 approach has been extensively used to derive ET and schedule irrigation on an operational basis. This approach is often preferred due to its simplicity and its robustness for operational applications. It requires fewer input data, and provides acceptable ET estimates when compared to heavily parameterized physically-based models (Evelt et al., 1995; Kite and Droogers, 2000; Eitzinger et al., 2002), to ground measurement (e.g. Paço et al., 2006; Er-Raki et al., 2007, 2008, 2009; Liu and Luo,

79 2010) or to satellite measurements (e.g. Allen, 2000; Kite and Droogers, 2000; Duchemin et
 80 al., 2006; Er-Raki et al., 2006, 2010). FAO-56 is based on the concepts of reference
 81 evapotranspiration ET_0 and crop coefficients K_c , which have been introduced to separate the
 82 climatic demand from the plant response (Allen et al., 1998). There are two approaches to
 83 estimate crop evapotranspiration: the single and the dual crop coefficients. The FAO-56 dual
 84 crop coefficient approach (Allen et al., 1998) describes the relationship between maximal
 85 evapotranspiration ET_c and reference evapotranspiration ET_0 by separating the single K_c
 86 into the basal crop K_{cb} and soil water evaporation K_e coefficients, while in the FAO-56
 87 single crop coefficient approach, the effect of both crop transpiration and soil evaporation are
 88 integrated into a single crop coefficient. Many studies have focused on the application of the
 89 single approach for determining olive water requirement within Mediterranean regions (e.g.
 90 Palomo et al., 2002; Abid Karray et al., 2008; Martinez-Cob and Faci, 2010). In semi-arid
 91 Mediterranean region of southern Morocco, Er-Raki et al. (2008) applied also the single
 92 approach over the same study site of this work, and they found that the approach
 93 overestimates AET by about 18% when using the crop coefficient suggested by Allen et al.
 94 (1998). Knowing that the flood irrigation is the most widely used method by the majority of
 95 the farmers in Morocco (as the case of our study site), which accompanied with a large
 96 amount of the water lost through direct soil evaporation (Yunusa et al., 1997), it is worthwhile
 97 to estimate this substantial amount. This can be achieved by partitioning ET into soil and plant
 98 components, which is the main objective of this present study. For the FAO-56 dual crop
 99 coefficient approach, it has been tested for many crops (bean, corn, and sugar beet) at
 100 Kimberly, Idaho (Allen et al., 1996) and tomato and cotton at Fresno, California by Itenfisu
 101 (1998). As reported by Allen (2000), the comparison between estimated and measured ET by
 102 precision weighing lysimeters in all situations gives an error less than 10% for daily ET
 103 estimates. Allen (1999) applied the FAO-56 procedure to a 200,000 ha irrigation project in

California to compare the estimated ET with that determined by water balance, and the results showed that despite the simplicity of the FAO model, estimates of ET were reasonable with a good accuracy (overestimation of 6%). Allen (2000) also applied his methodology to an extensive multiple-cropped surface, and compared the estimated ET with one obtained by remote sensing. Results have shown that the FAO-56 approach overestimated ET by more than 20%. Recently, several studies used the FAO-56 dual crop coefficient for estimating water consumptions of different crops (Allen et al., 2005 a, b; Hunsaker et al., 2003, 2005; Paço et al., 2006; Er-Raki et al., 2007). Some of these studies adopted the FAO-56 dual approach to use satellite based vegetation index (Hunsaker et al., 2003, 2005; Er-Raki et al., 2007; González-Dugo and Mateo, 2008; Er-Raki et al., 2010). The results show that relating the basal crop coefficient K_{cb} to remotely sensed vegetation index greatly improves the performance of FAO-56 method. However, Er-Raki et al. (2006) showed that the performance of the FAO-56 method has some limitations when there is high soil evaporation or when stress occurs. To overcome this problem and then enhance the FAO-56 performances, ET derived from thermal infrared (TIR) observations was assimilated into FAO-56 single source model (Er-Raki et al., 2008) in order to estimate accurately the water consumption of olive orchards in the semi-arid region of the Tensift basin (central of Morocco).

Several studies have been specifically dedicated to estimate ET over olive trees. Villalobos et al. (2000) determined olive ET by the estimation of its two components, through a combination of a transpiration model based on the equation of Penmann-Monteith (Monteith, 1965) and a soil evaporation model similar to that of Ritchie (1972). Palomo et al. (2002) used a water balance approach, to determine water consumption in olive orchards. Among the several disadvantages of this approach, summarized by Fernández and Moreno (1999), is the variability of the hydraulic properties of the soil profile, such as the hydraulic conductivity-soil water content relationship. Recently, Testi et al. (2004) used the eddy-

covariance technique to obtain direct estimates of ET of young irrigated olive orchards in southern Spain. In the context of SudMed project (Chehbouni et al., 2008), Williams et al. (2004) used the sap flow method combined with the isotopic method to estimate plant transpiration and soil evaporation over olive orchards in southern Morocco.

Estimating total ET over olive orchards has been investigated by many studies in semi arid regions (e.g. Fernández et al., 2001; Testi et al., 2004; Ezzahar et al., 2007; Er-Raki et al., 2008), but there is little information on the partitioning of the relevant components of ET in such areas; this is one of the most important ecohydrological challenges in understanding water exchange and vegetation dynamics in arid and semi arid ecosystems (Reynolds et al., 2000; Huxman et al., 2005). Partitioning ET is possible by using a combination of micro-meteorological measurements (e.g. Bowen ratio, eddy covariance system), and eco-physiological techniques (e.g. sap flow, stable isotopes) (Williams et al., 2004; Yepez et al., 2005; Scott et al., 2006). However, these methods are expensive and difficult to deploy and maintain in both time and space. Recently, Moran et al. (2009) developed an operational approach for partitioning ET with a minimal cost and suitable for operation over long time periods. This approach is based on the difference between the mid-afternoon and pre-dawn soil surface temperature, which is considered as the indicator of the soil evaporation. In the same context, the present study aims to use an operational model of FAO-56 dual crop coefficient approach for partitioning ET. We first compared actual ET derived from this approach to that measured using an eddy covariance device, then the issue of the ability of this approach to provide accurate estimates of components of AET through a comparison of field data obtained from a combination of eddy covariance based AET measurements and spatialized or scaled-up sap flow measurements of transpiration. In this context the objectives of this study were:

1. to analyze the ability of the FAO-56 dual crop coefficient model to reproduce the temporal evolution of evapotranspiration and its components: plant transpiration and soil evaporation. Actual plant transpiration was compared with scaled-up sap flow measurements.
2. to estimate the most adequate water quantity needed for the olive and to determine the best timing of irrigation by using the FAO-dual approach.

This paper is organized as follows. Section 2 presents a description of study site and data collected during the 2003 and 2004 growing season. In Section 3, we provide a brief theoretical overview of the FAO-56 dual crop coefficient approach. Section 4 presents an application of this approach over an olive site. Also in this section, we analyze the ability of this approach to reproduce the temporal evolution of both components of evapotranspiration (plant transpiration and soil evaporation), and to derive the soil water stress coefficient K_s of olives orchards during growing season in order to determine the best timing of irrigation. In the final section, summary and conclusion are provided.

2. Experimental Data

The experimental data used for this research are similar to those used in the previous paper (Er-Raki et al., 2008). Here, we presented briefly the site description, climatic and eddy covariance measurements. However, as the main objective of this work is the partitioning of actual evapotranspiration (AET) into plant transpiration and soil evaporation through a combination of eddy covariance and scaled-up sap flow measurements, more detailed presentation of sap flow measurements and its scaled-up to stand level transpiration, which is not used in a previous paper (Er-Raki et al., 2008), is required.

2.1. Site description

This study was carried out during 2003 and 2004, in the Agdal olive (*Olea europaea* L.) orchard located in the semi-arid region of the Tensift basin, south-east of Marrakech,

Morocco (31.601 N, 7.974 W). This area has a mean total annual precipitation of 240mm and a corresponding mean annual reference evapotranspiration of 1600 mm. The average annual temperature is about 22°C, rising to 38 °C in the summer (July-August) and going down to 5 °C in winter (December-January). Mean seasonal wind speed was about 1.2 m/s. The experimental field is almost flat, planted with 240-year old olive trees, grown in an orchard of about 275 ha. The density of olive trees was about 225 trees per hectare, which provides an area of about 45 m² occupied by each tree. The soil type is homogeneous, with silt clay loamy texture (30% clay, 25% silt, and 44% sand). The groundwater depth is approximately 40 m. The soil surface was partly covered (\approx 20%) by natural grass (under story) consisting mainly of short weeds during most of the year. More details about the site description are given in Williams et al. (2004) and Er-Raki et al. (2008).

2.2. Data description

2.2.1. Meteorological data and eddy covariance measurements

All climatic parameters (solar radiation, air temperature, relative humidity and wind speed), needed for estimate daily reference evapotranspiration (ET_0) by the FAO-Penman Monteith (Equation 6 in FAO-56, Allen et al., 1998) are measured. More details about the instruments (type, position) used for measurements of these parameters collected over our study site are provided in Er-Raki et al. (2008).

Figure 1 reports the daily pattern of ET_0 calculated by the FAO-Penman-Monteith equation for the two olive growing seasons (2003 and 2004). The temporal evolution of ET_0 during the year is typically that of a semi-arid continental climate. It is characterised by a high climatic demand, with the lowest during rainy periods (winter) and the highest values occurred in the sunny days (summer). Precipitation temporal patterns over the growing season of olive trees were characterized by low and irregular rainfall events, with a total precipitation amount of about 280 mm (Figure 1). The amount and timing of irrigations applied by the

farmer are presented also in this figure. It was about 800 mm for each season (2003 and 2004) of olives with around 100 mm in each supply. This irrigation scheme used by the farmer has been evaluated in this study.

In addition to climatic measurements, an eddy covariance system, constituted with a 3D sonic anemometer (CSAT3, Campbell Scientific Ltd.) and an open-path infrared gas analyzer (Li7500, Licor Inc.), was installed over olive tree to provide continuous measurements of vertical fluxes of heat and water vapour at 9.2 m. A detailed description of eddy covariance measurements can be found in Ezzahar et al. (2007) and Er-Raki et al. (2008). As reported also in the same papers, the approximate fetch (spatial scale) of evapotranspiration measurement is about 40m in the northwestern direction. It might be considered adequate as it contributed 90% of the measured sensible heat flux (Hoedjes et al., 2007) and it includes the trees where the sap flow measurements were taken. Data sets of latent heat and sensible heat fluxes have been available during 2003 and 2004 growing seasons of olive orchards. Missing data in some days is associated to the collapse of power supply.

The evaluation of the flux measurements is undertaken through the analyzing the energy balance closure. By ignoring the term of canopy heat storage and the radiative energy used in photosynthesis (Testi et al., 2004; Baldocchi et al., 2000), the energy balance closure is defined as:

$$R_n - G = H_{EC} + L_v E_{EC} \quad (1)$$

Where R_n is the net radiation; G is the soil heat flux; H_{EC} and $L_v E_{EC}$ are respectively the sensible heat flux and the latent heat flux measured by eddy covariance system. Figure 2 shows how well the available energy ($R_n - G$) was balanced by ($H_{EC} + L_v E_{EC}$) at daily time scale for the 2003 and 2004 growing season of olive orchards. The slope of the regression forced through the origin was 1.06 in 2003 and 1.07 in 2004, indicating an underestimation of

the flux ($H_{EC} + L_v E_{EC}$) was less than 10% of the available energy ($R_n - G$), with the Root Mean Square Error (RMSE) being about 17 W.m^{-2} in 2003 and 19 W.m^{-2} in 2004 (the equation used to calculate RMSE is presented in Appendix). These results indicate --at least at the daily time scale-- a good closure of the energy balance, which is in agreement with other studies (Testi et al., 2004; Baldocchi et al., 2000; Twine et al., 2000).

2.2.2. Sap flow measurements

Heat-pulse sap flow sensors (Heat Ratio Method, HRM, Burgess et al., 2001) were used to measure xylem sap flux on eight olive trees. The HRM method has been described in detail in Burgess et al. (1998) and Burgess et al. (2001). Briefly, the HRM is a modification of the Heat Pulse Method (HPM) and it employs temperature probes inserted into the active xylem at equal distances down- and upstream from a heat source. This method improves on the HPM by its precision at very slow flow rates and even reverses sap flow can be measured. Reliability of this technique for determining transpiration has been demonstrated by several studies (Burgess et al., 2001; Fernández et al., 2001 and Williams et al., 2004). The heat pulse sensors were installed on four large single-stemmed and on four large multi-stemmed trees adjacent to the eddy covariance tower during the summer of 2003 and 2004. Sap flow measurements were conducted from the 14th of June (DOY 165) through the 30th of July (DOY 211) during 2003 and from the 9th of May (DOY 130) through the 28th of September (DOY 272) during 2004. Missing data in some days (from DOY 183 to DOY 194 and from DOY 222 to DOY 224) is due to problems with the power supply. The same measurements of sap flow, with the same sensors and over the same field have been made by Williams et al. (2004) except in other climatic conditions (during the winter). A detailed description of HRM technique and the principle of measurements can be found in Williams et al. (2004). Volumetric sap flow (L day^{-1}) was scaled to tree transpiration (mm day^{-1}) using a survey of the average ground area of each tree (45 m^2). After the scaling the measured sap flow to the

single tree transpiration, we extrapolated this latter to the stand level transpiration, which is representative for the whole field. The allometric method is the most one used for this up scaling (e.g. Kumagai et al., 2005; Ford et al., 2007). However, this method is destructive and very time-consuming. Nevertheless, in this study the extrapolation of the tree transpiration to the stand level transpiration has been performed based on the measurements of eddy covariance. This strategy was also proposed by Williams et al. (2004) and Oishi et al. (2008) in the context of scaling ecosystem-level transpiration from sap flux measurements based on the measured AET by eddy covariance system. In the same context, we tried to find the relationship between the scaled measured sap flow and measured AET by eddy covariance, equivalent to tree level transpiration, during the dry conditions (when the soil evaporation is negligible). In order to select the dry period, daily evolution of $\Delta\theta$ was plotted from DOY 195 to DOY 219 (Figure 3), when $\Delta\theta$ means the difference between the soil moisture at 5 cm depth on day i and on day i-1. One assumes that $\Delta\theta$ is proportional to the soil evaporation flux at least several days after a major irrigation, i.e. when the excess water has been redistributed within the soil moisture profile. By analysing this figure, one can see that $\Delta\theta$ increased in absolute value from DOY 195 to DOY 202, and after it decreased until DOY 212. After this day, $\Delta\theta$ is almost constant and close to zero. Therefore, the soil moisture ($0.13 \text{ m}^3/\text{m}^3$) correspond to DOY 212 was considered as the threshold which can be the indicator of the presence of soil evaporation. When the soil moisture at 5 cm is lower than this threshold, the soil evaporation is considered negligible regarding the large values of ET_0 during the summer. After the selection of the dry conditions, measured daily AET by eddy covariance system was plotted against the daily scaled sap flow measurements (data not presented here). Then, the obtained linear regression between daily stand level transpiration and daily scaled sap flow is:

$$\text{Stand level transpiration} = 1.25 * (\text{scaled sap flow}), \quad R^2 = 0.74 \quad (2)$$

This model was applied also for the remaining days (wetting days) of sap flow measurements for calculating the stand level transpiration. This may create some errors in estimating stand level transpiration as reported by Oishi et al. (2008) when they found that the agreement between the estimates of components AET is greatly affected by the scaling procedure.

3. Theoretical overview of the FAO-56 dual approach

Detailed descriptions of the FAO-56 dual crop coefficient approach are available from Allen et al. (1998). In this section, we will briefly present this approach. The actual crop evapotranspiration (AET) estimated by this approach is given by the following equation:

$$AET = (K_s K_{cb} + K_e) ET_0 \quad (3)$$

Where K_{cb} , K_e and K_s are basal crop coefficient, soil evaporation and water stress coefficient, respectively. The required equations for deriving these three parameters are presented henceforth.

3.1. Calculation of K_{cb}

The methodology adopted here to compute basal crop coefficient (K_{cb}) follows strictly the same method displayed in Er-Raki et al. (2008) for calculating crop coefficient (K_c). As mentioned previously in the introduction, two different crops (olives and under story) grew up together in the same field. A simple formula was used to calculate the equivalent basal crop coefficient (Allen et al., 1998):

$$K_{cbfield} = f_{c-olives} K_{cbngc} + (1 - f_{c-olives}) K_{cbcov er} \quad (4)$$

Where K_{cbngc} and $K_{cbcov er}$ are basal crop coefficients for olive and under story, respectively. The average seasonal value of basal crop coefficient of olive orchards (K_{cbngc}) was derived based on sap flow measurements. For the basal crop coefficient of under story

301 ($K_{cb\ cov\ er}$), it was assumed equal to the difference between the ratio of measured AET and ET_0

302 ($K_c = \frac{AET}{ET_0}$) and K_{cbngc} during the dry conditions. $f_{c-olives}$ is the fraction of soil surface

303 covered by olive trees, calculated as $f_{c-olives} = \frac{\pi D^2 N}{40000}$ where D (m) is the average diameter of

304 the canopy and N is the number of trees per hectare. It was found to be equal to about 0.60.

305 **3.2. Calculation of K_e**

306 This coefficient is calculated based on daily computation of the water balance for the

307 surface soil evaporation layer Z_e (equation 71 in FAO-56 paper). The calculation procedure

308 requires input of soil parameters such as the soil moisture at field capacity (θ_{fc}) and at the

309 wilting point (θ_{wp}), the total evaporable water (TEW), the readily evaporable water (REW)

310 and the depth of Z_e . An average value of $0.32\ m^3\ m^{-3}$ for θ_{fc} and $0.19\ m^3\ m^{-3}$ for θ_{wp} were

311 obtained (Er-Raki et al., 2008). For the depth of the soil surface evaporation layer Z_e (m),

312 Allen et al. (1998) suggested values ranging between 0.10 and 0.15 m. Because the soil is

313 covered with herbs and is shaded by trees, the value of $Z_e = 0.15\ m$ is adopted in this study. A

314 typical REW value for a silt clay loamy soil of 9 mm (FAO-56, table19) was used in the

315 calculations. Another parameter is needed for the calculation of K_e . This parameter is named

316 the exposed and wetted soil fraction (f_{ew}). It was derived following the suggestions of Allen

317 et al. (1998) (equation 75 in FAO-56 paper). In fact, following irrigation (flooding technique)

318 or rainfall, the soil was completely wetted except the area covered by the stem ground tree.

319 This area represents about 5% of the whole area occupied by each tree. Then, the fraction of

320 soil surface wetted by irrigation or precipitation f_w was about 0.95 and f_{ew} was equal to (1-

321 f_c). In the absence of the rainfall and irrigation, it was equal to $f_w \cdot f_c$. f_c represents the fraction

322 of soil surface covered by olive trees and understory, which it was set at 0.80.

3.3. Derivation of K_s

When the dual crop coefficient approach is adapted, the effects of soil water stress on crop AET are accounted by multiplying the basal crop coefficient by the water stress coefficient, K_s . Mean water content of the root zone is expressed by the root zone depletion, D_r . At field capacity, the root zone depletion is zero ($D_r = 0$). Water stress occurs when D_r becomes greater than RAW , the depth of readily available water in the root zone. For $D_r > RAW$, K_s is given by:

$$K_s = \frac{TAW - D_r}{TAW - RAW} = \frac{TAW - D_r}{(1-p)TAW} \quad (5)$$

Where K_s is a dimensionless transpiration reduction factor dependent on available soil water [0–1], D_r is root zone depletion [mm], TAW is total available soil water in the root zone [mm], and p is the fraction of TAW that a crop can extract from the root zone without suffering water stress. When $D_r \leq RAW$; $K_s = 1$.

TAW is estimated as the difference between the water content at field capacity and wilting point:

$$TAW = 1000 \left(\theta_{fc} - \theta_{wp} \right) Z_r \quad (6)$$

Where Z_r is the effective rooting depth [m].

Readily available soil water of the root zone is estimated as:

$$RAW = pTAW \quad (7)$$

The required soil parameters for calculation of K_s are taken from Er-Raki et al. (2008). TAW and RAW values calculated from equation (6) and (7) are 208 and 135.2 mm, respectively. The rooting depth Z_r of olive trees and the depletion fraction p were set at 1.60 m and 0.65 respectively, according to FAO-56 values (table 22).

4. Results and discussions

4.1. Estimating AET by the FAO-56 dual crop coefficient approach

We calculated the variation over time of actual evapotranspiration (AET) using the FAO-56 dual crop coefficient approach over olive trees during two consecutive growing seasons (2003 and 2004). The simulation was performed from March, 1st (DOY 60) to November, 25th (DOY 329) for 2003, and from the March, 1st (DOY 61) to November, 7th (DOY 312) for 2004. The average seasonal value of basal crop coefficient of olive orchards used for the simulation was about 0.54. This value was derived based on sap flow measurements during 2003. It was expressed as the ratio of measured transpiration by sap flow to the reference evapotranspiration ET_0 . When sap flow measurements are not available, basal crop coefficient has been derived based on minimum values of measured crop coefficient (ratio of measured AET to ET_0) according to Teixeira et al. (2008). The comparison between measured and predicted AET (figure 4) shows good agreement between observed and simulated AET values. The Root Mean Square Error (RMSE) between measured and simulated AET values during 2003 and 2004 were respectively about 0.54 and 0.71 mm per day. Some discrepancies between measured and simulated AET can be clearly observed around wetting events (irrigation and rainfall) and stress period. For wetting events, the difference between measured and simulated AET values may be due to the deep percolation and the rainfall interception, which not taken into account by the model. As reported by Gomez et al. (2001), rainfall interception plays an important component of the water balance, and they showed that the water intercepted by the rainfed olive orchards was about 8% for a heavy rainfall. Another factor that may partly explain some of the difference between measured and simulated AET values is the flux source area measured by eddy covariance which depends to the wind direction. In fact, the eddy covariance system measures the evapotranspiration over a relatively large area (wet and dry) whereas the model simulates

it locally (wet or dry). Moreover, the dual approach tends to overestimate the crop evapotranspiration at the peak values (wetting events). This is corroborated by Liu and Luo (2010) when they found that the dual approach of FAO-56 is appropriate for simulating the total quantity of evapotranspiration but inaccuracy in simulating the peak value after precipitation or irrigation (Peng et al., 2007). This necessitates a more profound study for improving some parameterisation used in the FAO-56 method. For the periods of hydric stress (ex. from DOY 212 to DOY 238 during 2004), the approach leads to higher values of AET in comparison with that measured by the eddy covariance system. This may be due to an overestimation of soil water stress coefficient. The overestimation of soil water stress can be related to the overestimation of the rooting depth (1.6 m). This misrepresentation of the rooting depth influences directly the ability of the plant to extract water. A similar result has been found when using the single approach for estimating water consumption for the same olive orchard (Er-Raki et al., 2008). To illustrate more clearly the effect of the rooting depth (Z_r) on evapotranspiration, it is essential to perform a sensitivity analysis of the FAO model to this parameter. The impact of rooting depth on AET (data not shown here) showed that the values of simulated AET increase with increasing of Z_r . In fact, an increase in Z_r causes an increase of Total Available Water (TAW) within the root zone and leads to an increase in the soil water stress coefficient K_s which is straightforward according to the equations (6) and (7). An increase in Z_r of 33.33%, 66.66%, and 166% (from 1.2 to 1.6, from 1.2 to 2 from 1.2 to 3.2 m, respectively) leads to an increase of AET by about 34%, 47% and 49%, respectively. Note that the effect of rooting depth on AET is negligible when the water is not limiting within the root zone.

According to this study, the FAO-56 dual crop coefficient approach simulates reasonably well the total evapotranspiration. The question addressed after is how efficiently

this approach simulates the two components individually: plant transpiration and soil evaporation.

4.2. Performance of the dual crop coefficient approach for Partitioning of evaporation and transpiration

The FAO-56 dual crop coefficient approach computes separately soil evaporation and plant transpiration; it is of interest to investigate how well these individual components are simulated. To achieve this objective, we combined eddy covariance based measurement of AET with scaled-up sap flow measurements to estimate soil evaporation and plant transpiration against which the simulated components will be compared. As stated above, sap flow measurements were conducted from DOY 130 to DOY 272 during 2004. The sum of measured soil evaporation and the under story transpiration was computed as the difference between AET measured by the eddy covariance and the olive transpiration measured by the sap flow method. For practical reasons, the heat pulse sensors were inserted only into the active xylem of olive trees. Therefore, we compared the simulated soil evaporation with the sum of measured soil evaporation and the under story transpiration. Also, because the FAO-dual approach predicts separately only soil evaporation and plant transpiration (olives + under story) and does not discriminate between the three components (soil evaporation, olive transpiration and under story transpiration), we compared the simulated plant transpiration with the measured olive transpiration only.

Figure 5a presents a comparison between the measured and simulated transpiration for the 2004 growing season. Daily patterns are very similar and respond to that of ET_0 (see Figure1-bottom). The RMSE between measured and simulated olive transpiration was about 0.59 mm per day. The cumulated values of the entire experimental period (128 days) are 362 mm for the transpiration measured by the HRM method and 387 mm for the model, leading to

a difference of 7%. This difference is consistent with the fact that the model simulates the olive transpiration and the under story transpiration while the measurement estimates only the olive transpiration. Another factor that may partly explain this difference is that the scaling approach (Eq. 2) is not error-free (Fernández et al., 2001; Williams et al., 2004).

Regarding soil evaporation, Figure 5b shows that in dry conditions (absence of irrigation and rainfall) both simulated and measured soil evaporation are almost zero. It should be noted that the observed negative values of measured soil evaporation are considered as an artefact and set to zero. After irrigation or rainfall, as expected, both measured and estimated soil evaporation increased. However the increasing magnitude is different. This error is likely due to the fact that:

- 1) the model simulate only soil evaporation, but the measurement gives the soil evaporation and under story transpiration;

- 2) the scaling approach of measured transpiration from the eddy covariance (Eq. 2) may not be valid in humid conditions and tends to underestimate the measured plant transpiration and thus overestimate soil evaporation, also this error can be related also to the under story contribution;

- 3) the impact of the difference in the footprint of the eddy covariance and the area where the measured sap flow was taken during the irrigation events. This may be underestimates or overestimates measured evaporation.

Despite those discrepancies between the measured and simulated soil evaporation, the model gives acceptable results in estimating soil evaporation. The RMSE between simulated and measured soil evaporation (+ under story transpiration) was 0.73 mm per day.

The ratio of plant transpiration and soil evaporation to total evapotranspiration (data not shown here) showed that before irrigation, plant transpiration represents 100% of total evapotranspiration and decrease to about 65% after irrigation. An amount of 35% of water

was lost by direct soil evaporation due to flooding irrigation and the olive trees are widely spaced. Another study was done over the same field by Williams et al. (2003, 2004) in winter. It showed that after the irrigation, the soil evaporation represents about 14–28% of the total evapotranspiration. Yunusa et al. (1997) also studied the partitioning of seasonal evapotranspiration from a commercial furrow-irrigated Sultana vineyard, and they found that substantial amounts of the soil water (about 49% of total ET) were lost through soil evaporation. In order to prevent the water losses by evaporation from the ground, it is very important to wet the maximum volume of root zone and the minimum soil surface. Therefore, a localized irrigation system is usually the most appropriate.

Despite the simplicity of the water balance model used in the FAO-56 formulation, the obtained results showed that the FAO-56 dual crop coefficient can simulate correctly crop evapotranspiration and gives also an encouraging result for partitioning of evapotranspiration into soil evaporation and plant transpiration. Because this approach is very simple and designed to schedule irrigation on an operational basis, it is of interest to check the irrigation planning practiced by the farmer over the study site. This can be achieved by applying the FAO model in order to determine when to irrigate and how much water to apply.

4.3. Assessment of irrigation planning

In order to assess the efficiency of the irrigation planning over the study site, we calculated the soil water stress coefficient K_s by the FAO-56 dual approach (Figure 6a). The soil water stress coefficient, K_s , for olive orchards ranges from 0 to 1 according to Equation (5), and it shows how the soil water depletion, D_r , changes to limit crop evapotranspiration. The value of K_s depends on the soil water depletion linked to water supply (rainfall or irrigation). The soil water stress is equal to 1 when the soil water depletion is less than the readily available water of the root zone (RAW). The absence of irrigation and rainfall (from

DOY 191 to DOY 237) results in an increase in the root zone depletion that exceeds *RAW* and generates stress (K_s below to 1). The increase in soil water depletion is due to the removal of water by evapotranspiration and percolation losses that induces water stress conditions. The information obtained from the soil water stress coefficient can be used in an irrigation scheduling program for deciding when and how much to irrigate. For this purpose, we used the FAO-56 dual approach to simulate the amount and the frequency of irrigation needed (figure 6a) for olive orchards in 2004 to avoid water stress (i.e. so that $K_s=1$ at all times). Following the FAO-56 procedure, irrigation is required when rainfall is insufficient to compensate the water lost by evapotranspiration. By calculating the soil water balance of the root zone on a daily basis (Equation 85 in FAO-56), the timing and the depth of the irrigations can be planned (Figure 6a). According to this figure, the average amount of irrigation in each supply was about 136 mm which corresponds to the value of *RAW*. The total irrigation recommended by the model was about 411 mm which it is half that given by the farmer (800 mm). It can be noticed also in this figure, that although the amount of irrigation given by the farmer was greater than the one simulated by the FAO model, the vegetation suffered from water stress during the summer (between DOY 228 and DOY 237). Such behaviour can be explained by inadequate distribution of irrigation: the wrong quantity is applied at the wrong moment. In fact, the farmer didn't apply the irrigation in this period while the model recommends the irrigation in the same period. It can be seen also that the farmer applied a large amount relatively to the required quantity given by the model. This is due to some unnecessary irrigation events during the rainfall period (e.g. DOY 169). The results revealed that the method of irrigation applied by the farmer was not appropriate for the olive orchards in the Tensift plain.

As we found above that an important amount of water ($\approx 35\%$) was lost by direct soil evaporation during the wetting event, it is of interest to quantify the amount of water needed

494 to fulfill this water depleted from the topsoil layer (Z_e). A similar parameter to K_s named soil
 495 evaporation reduction coefficient (K_r) was deployed to schedule irrigation in the topsoil layer
 496 (Allen et al., 1998). Similarly to K_s , the estimation of K_r requires a daily water balance
 497 computation but for the surface soil evaporation layer Z_e . Figure 6b presents the evolution of
 498 K_r with the timing and the amount of irrigation required. According to this figure, K_r varied
 499 between 0 and 1 depending to the amount of water available in the topsoil. Following heavy
 500 rainfall or irrigation, the evolution of K_r or soil evaporation rates can be described as two-
 501 stage process: an energy limiting stage, and a falling rate stage. In the first stage, the soil
 502 surface remains wet, the amount of water depleted by evaporation is equal to 0 and K_r is equal
 503 to 1. When the water content was reduced due to the depletion of water by evaporation
 504 (second stage) with the absence of rainfall and irrigation, K_r decreases and reaches 0 when the
 505 total evaporable water (TEW) was totally depleted. In this second stage, the soil evaporation
 506 rate decreases depending to the amount of water remaining in the surface soil layer and the
 507 soil hydraulic properties that determine the transfer of liquid and vaporized water to the
 508 surface. Ritchie (1972) funded that in the second stage the evaporation rate decreases as a
 509 function of the square root of time after wetting event. Based on the calculation of K_r by using
 510 the water balance equation (equations 74 and 77 in FAO 56), the timing and the amount of
 511 irrigations needed in the topsoil layer can be planned (Figure 6b) in order to compensate the
 512 water depleted from the topsoil layer (Z_e). According to this figure, the irrigation is required
 513 by FAO when the soil water depletion is higher than the readily evaporable water (REW) and
 514 no irrigation otherwise. The average value of irrigation recommended by FAO model in each
 515 supply was about 9 mm which corresponds to the value of REW except in the beginning of the
 516 calculation where it would be assumed as the total evaporable water ($TEW=33.55$ mm). The
 517 total amount of irrigation recommended by the FAO model for maintaining soil wet was about
 518 186 mm, which presents about 45% of the irrigation needed (411 mm) for avoiding olive

water stress. The cumulated values of total irrigation in the topsoil and in the root zone are about 597 mm for the simulated irrigation requirement by the FAO model and 800 mm for that given by the farmer, with a difference of 25%. This difference may be related to the inadequate amount and planning of irrigation by the farmer. Water amounts and timing are planned only by the understanding and perception of the farmer without using any guideline for scheduling the amount and timing of irrigation water applications. Consequently, some irrigations are missing or unnecessary. For example on DOY 201 (July, 19), the model recommends the irrigation while the farmer didn't apply it in this day. Effectively, in this period, the irrigation is needed because the climatic demand was very higher in the summer. During the rainfall period (e.g. DOY 169), the irrigation is not necessary, but the farmer apply one. The results revealed that the method of irrigation applied by the farmer was not appropriate for the olive orchards in the Tensift plain. It would be advisable to improve the irrigation management and to recommend the farmer to use the simple FAO model, which can be considered as a potentially useful tool for planning irrigation schedules on an operational basis.

5. Conclusions

The main objective of this study was to investigate the potential of the FAO-56 dual crop coefficient approach to provide accurate estimates of actual evapotranspiration (AET) and its components of the olive orchard in semi-arid region. Model simulations of evaporation and transpiration were compared to data obtained from a combination of eddy covariance based AET measurements and scaled-up sap flow measurements of transpiration.

The results showed that, by using the local values of basal crop coefficients derived from sap flow measurements, the approach simulates reasonably well AET over two growing seasons. The Root Mean Square Error (RMSE) between measured and simulated AET values during 2003 and 2004 were respectively about 0.54 and 0.71 mm per day. The value of basal

crop coefficient for the olive orchard used in this study was about 0.54. This value was lower than that suggested by the FAO-56 (0.62).

Since the FAO-56 dual crop coefficient approach predicts separately soil evaporation and plant transpiration, an attempt of comparison of the simulated components of evapotranspiration (soil evaporation and plant transpiration) with the measurements showed that the model gives an acceptable estimate of plant transpiration and soil evaporation. The RMSE between measured and simulated transpiration and soil evaporation (resp) were 0.59 and 0.73 mm per day. In conclusion, it can be stated that the FAO-56 dual crop coefficient gives an encouraging result for partitioning of evaporation and transpiration despite the simplicity of the formulation used to derive such partition. Further effort will be necessary if more accurate simulation of ET partitioning is needed by this approach. This can be achieved by subdividing the plant transpiration into olive transpiration and understory transpiration and so two water balance are necessary for calculation stress coefficient K_s .

Additionally, the results of this study revealed that the irrigation scheme used by the farmer was not appropriate for the olive orchards in the Tensift plain. It was found that although the amount of irrigation applied by the farmer (800 mm) during the growing season of olive orchards was greater than the simulated one by the FAO model (411 mm), the vegetation suffered from water stress especially during the summer. Such behaviour can be explained by inadequate distribution of irrigation. It would be advisable to improve the irrigation management and to recommend the farmer to use the simple and operational FAO model for planning irrigation schedules.

6. Acknowledgements

This study was supported by SUDMED (IRD-UCAM) and PLEADeS projects funded by the European Union (PCRD). The authors are grateful to ORMVAH (*‘Office Regional de Mise en Valeur Agricole du Haouz’*, Marrakech, Morocco) for its technical help. We thank the

director and staff of the Agdal olive orchard for access and use of the field site and for assistance with irrigation scheduling and security.

7. Appendix

Three statistics were used for analyzing the data: 1) the Mean Bias Error (MBE), which indicates the average deviation of the predicted values from the measured values; 2) the Root Mean Square Error (RMSE), which measures the discrepancy of predicted values around observed values; 3) the efficiency (E), which judges the performances of simulation data.

$$MBE = \bar{y}_{mod} - \bar{y}_{obs}$$

$$RMSE = \sqrt{\frac{1}{n} \sum_{i=1}^n (y_{i\ mod} - y_{i\ obs})^2}$$

$$E = 1 - \frac{\sum_{i=1}^n (y_{i\ mod} - y_{i\ obs})^2}{\sum_{i=1}^n (y_{i\ obs} - \bar{y}_{obs})^2}$$

Where \bar{y}_{mod} and \bar{y}_{obs} are the averages of simulations and observations, n is the number of available observations, $y_{i\ mod}$ and $y_{i\ obs}$ are daily values of modeled and observed variables respectively.

8. References

Abid Karray, J., Lhomme, J.P., Masmoudi, M.M., Ben Mechlia, N. 2008. Water balance of the olive tree–annual crop association: A modeling approach. *Agric. Water Manage.* 95, 575-586.

587 Allen, R.G. 1996. Assessing integrity of weather data for use in reference evapotranspiration
588 estimation. *J. Irrig. Drain Eng.* ASCE 122 (2), 97-106.

589 Allen, R.G., Pereira, L.S., Raes, D., Smith, M. 1998. Crop Evapotranspiration—Guidelines
590 for Computing Crop Water Requirements, Irrigation and Drain, Paper No. 56. FAO, Rome,
591 Italy, 300 pp.

592 Allen, R.G. 1999. Concept paper—accuracy of predictions of project-wide evapotranspiration
593 using crop coefficients and reference evapotranspiration in a large irrigation project. In:
594 Proceedings of the United States Committee on Irrigation and Drainage Conference on
595 “Benchmarking Irrigation System Performance Using Water Measurement and Water
596 Balances”, San Luis Obispo, CA, 10–13 March 1999.

597 Allen R.G. 2000. Using the FAO-56 dual crop coefficient method over an irrigated region as
598 part of an evapotranspiration intercomparison study. *J. Hydrol.* 229, 27–41.

599 Allen, R.G., Pereira, L.S., Smith, M., Raes, D, and Wright, J.L. 2005a. FAO-56 dual crop
600 coefficient method for estimating evaporation from soil and application extensions. *J. Irrig.*
601 *Drain Eng.* ASCE 131 (1), 2-13.

602 Allen, R.G., Clemmens, A.J., Burt, C.M., Solomon, K, and O’Halloran, T. 2005b. Prediction
603 accuracy for project-wide evapotranspiration using crop coefficient and reference
604 evapotranspiration. *J. Irrig. Drain Eng.* ASCE 131 (1), 24-36.

605 Baldocchi, D.D., Law, B.E., Anthoni, P.M. 2000. On measuring and modeling energy fluxes
606 above the floor of a homogeneous and heterogeneous conifer forest. *Agric. For. Meteorol.*
607 102, 187–206.

608 Boulet, G., Chehbouni, A., Braud, I., Vauclin, M., Haverkamp, R., Zammit, C. 2000. A
609 simple water and energy balance model designed for regionalization and remote sensing data
610 utilization. *Agric. For. Meteorol.* 105, 117–132.

611 Braud, I., Dantas-Antonino, A.C., Vauclin, M., Thony, J.L., Ruelle, P. 1995. A simple soil-
612 plant-atmosphere transfer model (SiSPAT) development and field verification. *J. Hydrol.* 166,
613 213–250.

614 Brisson N., Mary B., Ripoche D et al. 1998. STICS: a generic model for the simulation of
615 crops and their water and nitrogen balances. I. Theory and parametrization applied to wheat
616 and corn. *Agron. J.* 18, 311-346.

617 Burgess S.S.O., M.A. Adams, N.C. Turner, and C.K. Ong. 1998. The redistribution of soil
618 water by tree root systems. *Oecologia.* 115, 306-311.

619 Burgess, S.S.O., Adams, M.A., Turner, N.C., Beverly, C.R., Ong, C.K., Khan, A.A.H., Bleby,
620 T.M. 2001. An improved heat pulse method to measure slow and reverse flow in woody
621 plants. *Tree Physiol.* 21, 589-598

622 Chehbouni, A., Escadafal, R., Duchemin, B., Boulet, G., Simonneaux, V., Dedieu, G.,
623 Mougnot, B., Khabba, S., Kharrou, H., Maisongrande, P., Merlin, O., Chaponnière, A.,
624 Ezzahar, J., Er-Raki, S., Hoedjes, J., Hadria, R., Abourida, A., Cheggour, A., Raibi, F., A.
625 Boudhar, A., Benhadj, I., Hanich, L., Benkaddour, A., Guemouria, N., Chehbouni, Ah.,
626 Lahrouni, A., Oliosio, A., Jacob, F., Williams, D. G., Sobrino, J. 2008. An integrated
627 modelling and remote sensing approach for hydrological study in arid and semi-arid regions:
628 the SUDMED Programme. *Int. J. Remote Sens.*, 29, 17 & 18, 5161 – 5181.

629 Duchemin, B., Hadria, R., Er-Raki S., Boulet, G., Maisongrande, P., Chehbouni, A.,
630 Escadafal, R., Ezzahar, J., Hoedjes, J., Karrou, H., Khabba, S., Mougnot, B., Oliosio, A.,
631 Rodriguez, J-C., Simonneaux, V. 2006. Monitoring wheat phenology and irrigation in Central
632 Morocco: on the use of relationship between evapotranspiration, crops coefficients, leaf area
633 index and remotely-sensed vegetation indices. *Agric. Water Manage.* 79, 1- 27.

634 Eitzinger J., Marinkovic D., Hösch J. 2002. Sensitivity of different evapotranspiration
635 calculation methods in different crop-weather models. In Rizzoli, A.E., Jakeman, A.J. (Eds.):

636 Integrated Assessment and Decision Support; Proc., 1st biennial meeting of the International
637 Environmental Modelling and Software Society (IEMSS), 24-27 June 2002, Lugano,
638 Switzerland. 2, 395-400.

639 Er-Raki, S., Chehbouni, A., Guemouria, N., Duchemin, B., Ezzahar, J., Hadria, R., BenHadj,
640 I. 2006. Driven FAO-56 dual crop coefficient approach with remotely-sensed data for
641 estimating water consumptions of wheat crops in a semi-arid region. The 2nd International
642 Symposium on Recent Advances in Quantitative Remote Sensing: RAQRS'II, 25-29
643 September 2006, Valencia, Spain.

644 Er-Raki S., Chehbouni G., Guemouria, N., Duchemin B., Ezzahar J., Hadria R.
645 2007. Combining FAO-56 model and ground-based remote sensing to estimate water
646 consumptions of wheat crops in a semi-arid region. *Agric. Water Manage.* 87, 41–54.

647 Er-Raki, S., Chehbouni, A., Hoedjes, J., Ezzahar, J., Duchemin, B., Jacob, F. 2008.
648 Improvement of FAO-56 method for olive orchards through sequential assimilation of
649 Thermal infrared based estimates of ET. *Agric. Water Manage.* 95, 309–321.

650 Er-Raki, S., Chehbouni, A., Guemouria, N., Ezzahar, J., Khabba, S., Boulet, G. and Hanich,
651 L. 2009. Citrus orchard evapotranspiration: Comparison between eddy covariance
652 measurements and the FAO 56 approach estimates. *Plant Biosys.* 143 (1), 201-208.

653 Er-Raki, S., Chehbouni, A., Duchemin, B. 2010. Combining satellite remote sensing data with
654 the FAO-56 dual approach for water use mapping in irrigated wheat fields of a semi-arid
655 region. *Remote Sens.* 2(1), 375-387.

656 Evett, S.R., Howell, T.A., Schneider, A.D., Tolk, J.A. 1995. Crop Coefficient Based
657 Evapotranspiration Estimates Compared with Mechanistic Model Results. In W.H. Espey, and
658 P.G. Combs (ed.). *Water resources engineering*, vol. 2, Proc. of the First International
659 Conference, Aug. 14-18 1995, San Antonio (Texas, USA).

660 Ezzahar J., Chehbouni, A., Hoedjes, J.C.B., Er-Raki, S., Chehbouni, Ah., Bonnefond, J-M.
 661 and De Bruin, H.A.R. 2007. The use of the Scintillation Technique for estimating and
 662 monitoring water consumption of olive orchards in a semi-arid region. *Agric. Water Manage.*
 663 89, 173-184.
 664 Fernández, J.E., Moreno, F., 1999. Water use by the olive tree. *Journal of Crop Production*. 2
 665 (2), 101–162.
 666 Fernández, J. E., M. J. Palomo, A. Díaz-Espejo et al. 2001. Heat-pulse measurements of sap
 667 flow in olives for automating irrigation: tests, root flow and diagnostics of water stress. *Agric.*
 668 *Water Manage.* 51, 99-123.
 669 Ford, C. R., Hubbard, R.M., Kloeppel, B. D, Vose, J. M. 2007. A comparison of sap flux-
 670 based evapotranspiration estimates with catchment-scale water balance. *Agric. For. Meteorol.*
 671 145, 176–185.
 672 Gómez, J. A., Giráldez, J. V. and Fereres E. 2001. Rainfall interception by olive trees in
 673 relation to leaf area. *Agric. Water Manage.* 49(1), 56-78.
 674 González-Dugo, M.P., Mateos, L. 2008. Spectral vegetation indices for benchmarking water
 675 productivity of irrigated cotton and sugarbeet crops. *Agric. Water Manage.* 95(1), 48-58.
 676 Hoedjes, J.C.B., Chehbouni, A., Ezzahar, J., Escadafal, R., De Bruin, H.A.R., 2007.
 677 Comparison of large aperture scintillometer and eddy covariance measurements: can thermal
 678 infrared data be used to capture footprint induced differences? *J. Hydrometeorol.* 8 (2), 144-
 679 159.
 680 Hunsaker, DJ., Pinter, PJ Jr., Barnes, EM., Kimball, BA. 2003. Estimating cotton
 681 evapotranspiration crop coefficients with a multispectral vegetation index. *Irrig. Sci.* 22, 95-
 682 104.
 683 Hunsaker, DJ., Pinter, PJ Jr., Kimball, BA. 2005. Wheat basal crop coefficients determined
 684 by normalized difference vegetation index. *Irrig. Sci.* 24, 1-14.

685 Huxman, T.E., Wilcox, B.P., Breshears, D.D., Scott, R.L., Snyder, K.A., Small, E.E., Hultine,
 686 K., Pockman, W.T., Jackson, R.B. 2005. Ecohydrological implications of woody plant
 687 encroachment. *Ecology*. 86, 308–319.

688 Itenfisu, D. 1998. Adaptation of resistance-based evapotranspiration functions to row crops.
 689 Unpublished PhD dissertation, Dept. Biol. and Irrig. Engng, Utah State Univ., Logan, UT,
 690 207pp.

691 Kite, G. W., Droogers P. 2000. Comparing evapotranspiration estimates from satellites,
 692 hydrological models and field data. *J. Hydrol.* 209, 3-18.

693 Kumagai, T., Nagasawa, H., Mabuchi, T., Ohsakia, S., Kubota, K., Kogia, K., Utsumi, Y.,
 694 Kogaa, S., Otsuki, K., 2005. Sources of error in estimating stand transpiration using allometric
 695 relationships between stem diameter and sapwood area for *Cryptomeria japonica* and
 696 *Chamaecyparis obtuse*. *Agric. For. Meteorol.* 206, 191–195.

697 Liu, Y., Luo, Y. 2010. A consolidated evaluation of the FAO-56 dual crop coefficient
 698 approach using the lysimeter data in the North China Plain. *Agric. Water Manage.* 97, 31-40.

699 Martinez-Cob, A., Faci, J.M. 2010. Evapotranspiration of an hedge-pruned olive orchard in a
 700 semiarid area of NE Spain. *Agric. Water Manage.* 97, 410-418.

701 Monteith, J. L. 1965. Evaporation and Environment. 19th Symposia of the Society for
 702 Experimental Biology, University Press, Cambridge, 19:205-234.

703 Moran, M.S., R.L. Scott, T.O. Keefer, W.E. Emmerich, M. Hernandez, G.S. Nearing, G.B.
 704 Paige, M.H. Cosh, P.E. O'Neill. 2009. Partitioning evapotranspiration in semiarid grassland
 705 and shrubland ecosystems using time series of soil surface temperature. *Agric. For. Meteorol.*
 706 149, 59-72.

707 Noilhan, J., Mahfouf, J.F. 1996. The ISBA land surface parameterisation scheme. *Global and*
 708 *Planetary Change*, 13:145-159.

709 Oishi, C.A., Oren, R., Stoy, P.C. 2008. Estimating components of forest evapotranspiration: A
710 footprint approach for scaling sap flux measurements. *Agric. For. Meteorol*, 148, 1719-1732.

711 Olioso, A., Chauki, H., Courault, D., and Wigneron, J.-P. 1999. Estimation of
712 evapotranspiration and photosynthesis by assimilation of remote sensing data into SVAT
713 models. *Remote Sens. Environ.* 68, 341–356.

714 Paço, T. A., Ferreira, M. I., Conceição, N. 2006. Peach orchard evapotranspiration in a sandy
715 soil: Comparison between eddy covariance measurements and estimates by the FAO 56
716 approach. *Agric. Water Manage.* 85, 305-313.

717 Palomo, M.J., Moreno, F., Fernandez, J.E., Diaz- Espejo, A., Giron, I.F. 2002. Determining
718 water consumption in olive orchards using the water balance approach. *Agric. Water Manage.*
719 55, 15-35.

720 Peng, S., Ding, J., Mao, Z., Xu, Z., Li, D., 2007. Estimation and verification of crop
721 coefficient for water saving irrigation of late rice using the FAO-56 method. *Transactions of*
722 *the CSAE* 23 (7), 30–34.

723 Reynolds, JF, Kemp, PR, Tenhunen, JD. 2000. Effects of long-term rainfall variability on
724 evapotranspiration and soil water distribution in the Chihuahuan Desert: a modeling analysis.
725 *Plant Ecology.* 150, 145–159.

726 Ritchie, J.T., 1986. The CERES-Maize model In: *CERES-Maize: Simulation model of maize*
727 *growth and development.* Ed by Jones C.A., and Kiniry J.R., Texas A M University press,
728 college station, Tx., (1986) 3-6.

729 Ritchie, J.T. 1972. Model for predicting evaporation from a row crop with incomplete cover.
730 *Water Resour. Res.* 8:1204-1213.

731 Scott, R.L., Huxman, T.E., Cable, W.L. and Emmerich, W.E. 2006. Partitioning of
732 evapotranspiration and its relation to carbon dioxide exchange in a Chihuahuan desert
733 shrubland. *Hydrol. Proces.* 20, 3227–3243.

734 Sinclair, T.R., and Seligman, N.G. 1996. Crop modeling: from infancy to maturity. *Agron. J.*
735 88, 698-704.

736 Teixeira, A.H. de C., Bastiaanssen, W.G.M., Moura, M.S.B., Soares, J.M., Ahmad, M.D.,
737 Bos, M.G. 2008. Energy and water balance measurements for water productivity analysis in
738 irrigated mango trees, Northeast Brazil. *Agric. For. Meteorol.* 148, 1524-1537.

739 Testi, L., Villalobos, F.J., Orgaz, F. 2004. Evapotranspiration of a young irrigated olive
740 orchard in southern Spain. *Agric. For. Meteorol.* 12, 1-18.

741 Twine, T.E., Kustas, W.P., Norman, J.M. et al. 2000. Correcting Eddy-Covariance Flux
742 Underestimates over a Grassland. *Agric. For. Meteorol.* 103, 279-300.

743 Villalobos, F.J., Orgaz, F., Testi, L., Fereres, E. 2000. Measurements and modeling of
744 evapotranspiration of olive (*Olea europaea* L.) orchards. *Eur. J. Agron.* 13, 155-163.

745 Williams, D.G., Cable, W., Hultine, K., Yepez, E.A., Er-Raki, S., Hoedjes, J.C.B., Boulet, G.,
746 de Bruin, H.A.R., Chehbouni, A. et Timouk, F. 2003. Suivi de la répartition de
747 l'évapotranspiration dans une oliveraie (*Olea europaea* L.) à l'aide des techniques de l'eddy
748 covariance, des flux de sève et des isotopes stables ». Vèmes Journées de l'Ecologie
749 Fonctionnelle, 12 au 14 Mars 2003 à Nancy.

750 Williams, D.G., Cable, W., Hultine, K., Hoedjes, J.C.B., Yepez, E.A., Simonneaux, V., Er-
751 Raki, S., Boulet, G., de Bruin, H.A.R., Chehbouni, A., Hartogensis, O.K. and Timouk, F.
752 2004. Evapotranspiration components determined by stable isotope, sap flow and eddy
753 covariance techniques. *Agric. For. Meteorol.* 125, 241-258.

754 Yepez, E.A., Huxman, T.E., Ignace, D.D., English, N.B., Weltzin, J.F., Castellanos, A.E. and
755 Williams, D.G. 2005. Transpiration and evaporation following a moisture pulse in semiarid
756 grassland: a chamber-based isotope method for partitioning evapotranspiration. *Agri. For.*
757 *Meteorol.* 132, 359–376.

758 Yunusa, I.A.M., Walker, R.R., Guy, J.R. 1997. Partitioning of seasonal evapotranspiration
759 from a commercial furrow irrigated Sultana vineyard. *Irrig. Sci.* 18, 45–54.

760

Figure captions

Figure 1. Daily reference evapotranspiration ET_0 calculated following the FAO-Penman-Monteith equation during 2003 (top) and 2004 (bottom) growing seasons. Rainfall and irrigation events are shown in the same figures.

Figure 2. Assessment of energy balance closure. Daily average fluxes of net radiation (R_n) minus the soil heat flux (G) are compared against the sums of sensible (H_{EC}) and latent heat ($L_v E_{EC}$) measured by the eddy covariance system.

Figure 3. Daily evolution of the difference between the soil moisture at 5 cm depth on day i and on day $i-1$ ($\Delta\theta$). The vertical dotted line shows the date on which the soil evaporation was negligible.

Figure 4. Time course of observed (triangles on dotted line) and simulated (solid line) actual evapotranspiration using the **FAO-56 dual crop coefficient approach** for 2003 (top) and 2004 (bottom) growing seasons of olives orchard in Tensift Alhaouz, Marrakech Morocco.

Figure 5. Time course of observed (triangles on dotted line) and simulated (solid line) two components of evapotranspiration using the FAO-56 dual crop coefficient approach of olives orchard in Tensift Alhaouz, Marrakech Morocco during the 2004 growing season (from DOY130 to DOY272): a) plant transpiration, b) soil evaporation. The measured soil evaporation is computed as the difference between measured evapotranspiration by eddy covariance system and measured transpiration by sap flow. Note that the negative values of measured soil evaporation obtained when the measured transpiration is higher than measured (AET) by eddy covariance system, were taken equal zero.

Figure 6. Estimated daily soil water stress coefficient K_s (figure a) and daily soil evaporation reduction coefficient K_r (figure b) by the FAO-56 dual crop coefficient approach for the olives orchard in Tensift Alhouz, Marrakech Morocco during 2004 growing season. Amount and

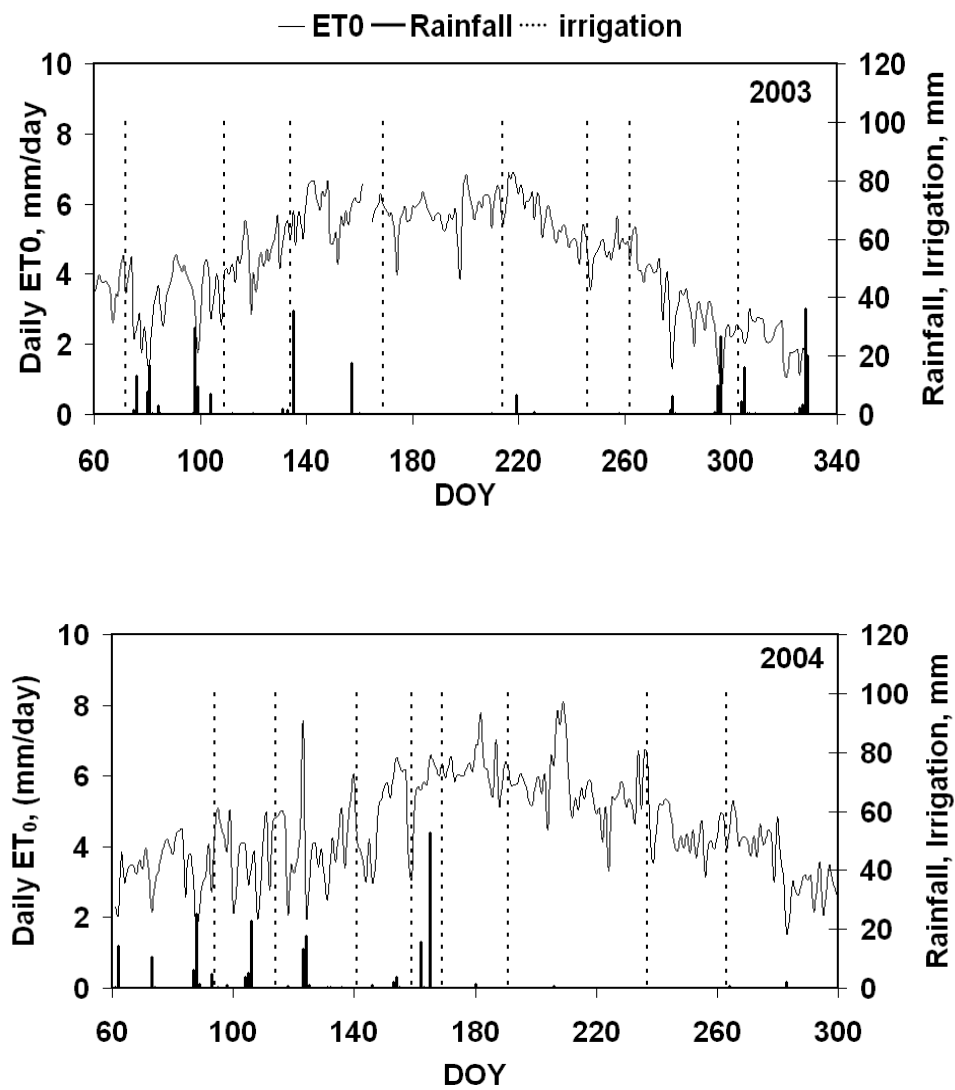
785 frequency of irrigation given by the farmer and recommended by the FAO model are shown
786 in the same figures.

787

788

789
790

Figure 1



791

792

793

794

795

796

797

Figure 2

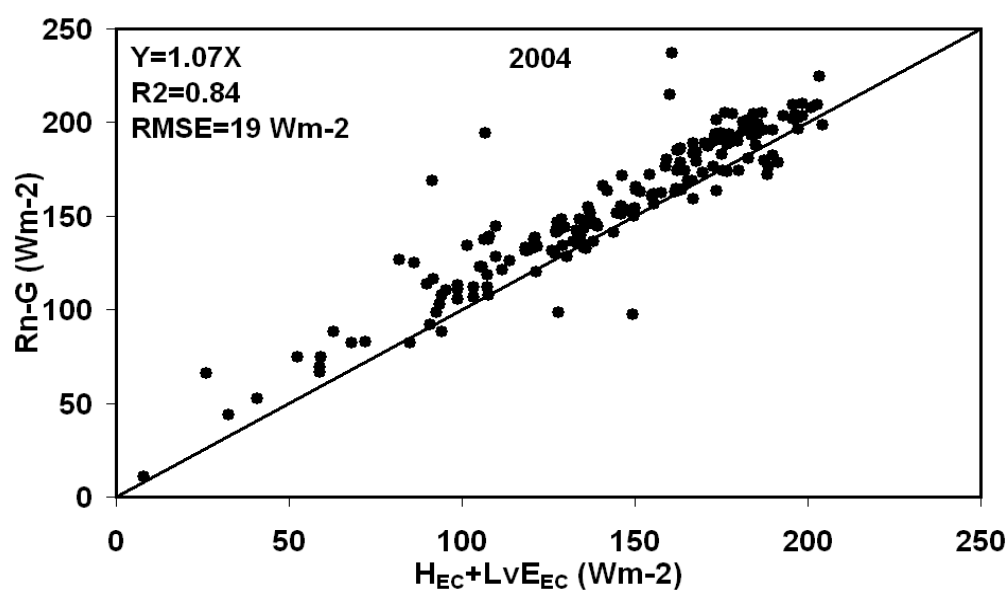
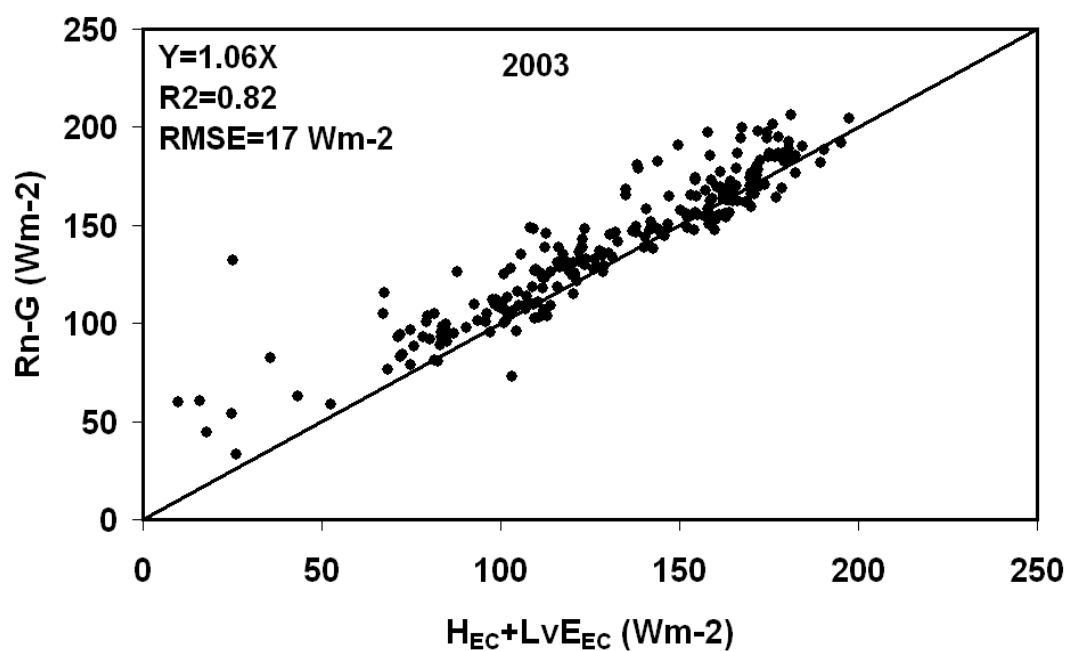
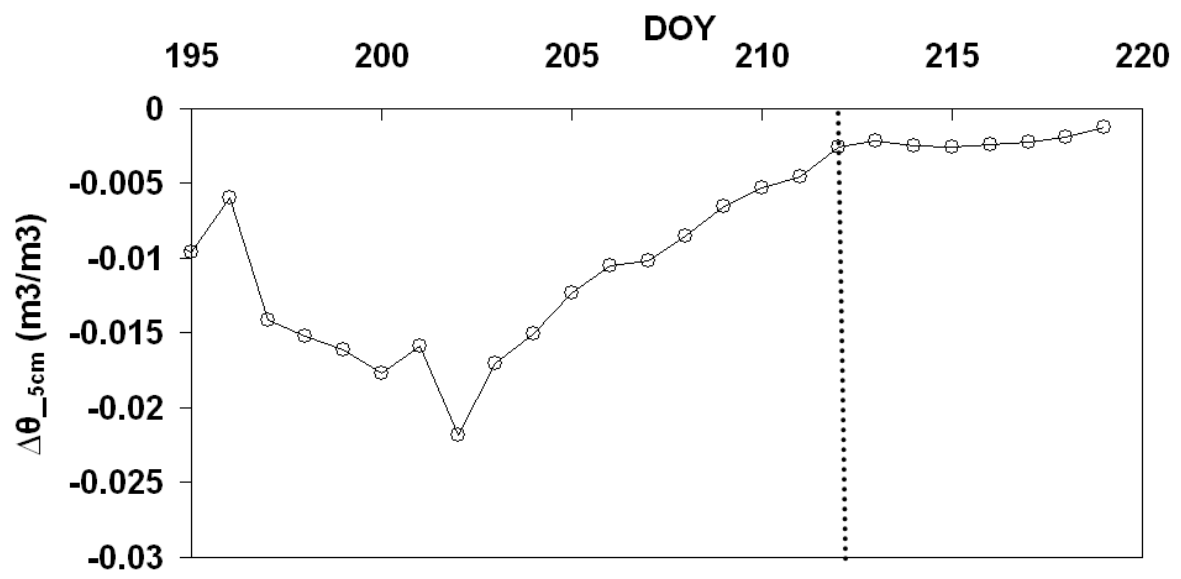
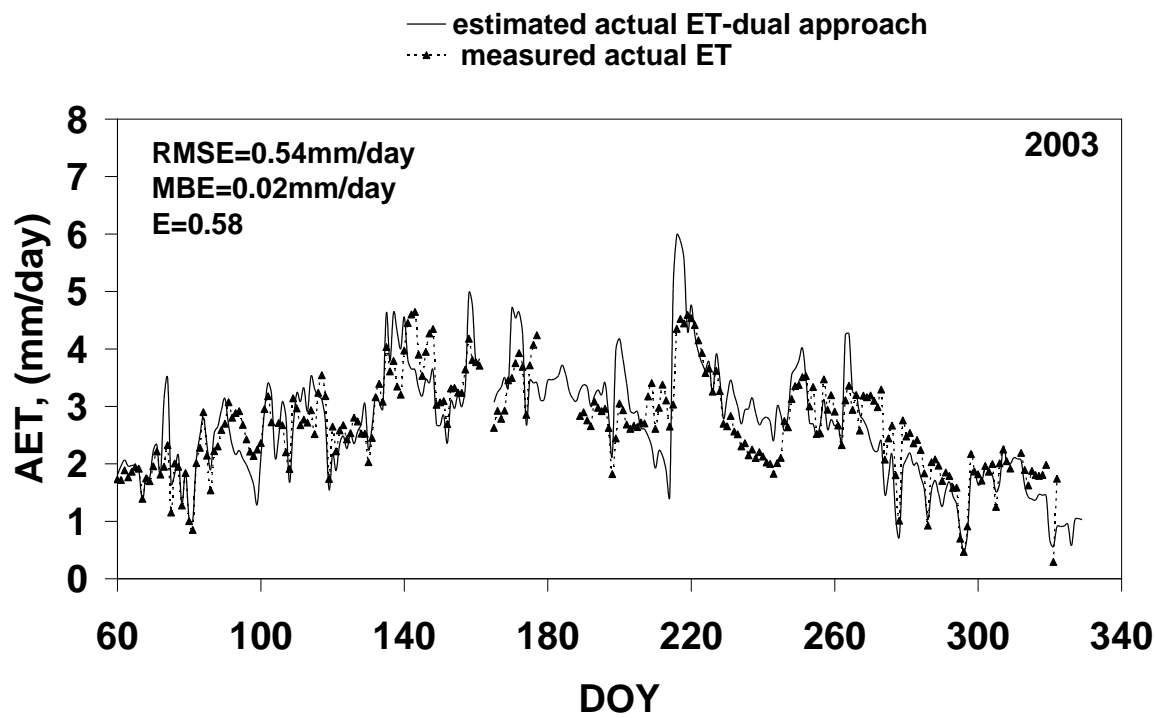


Figure 3

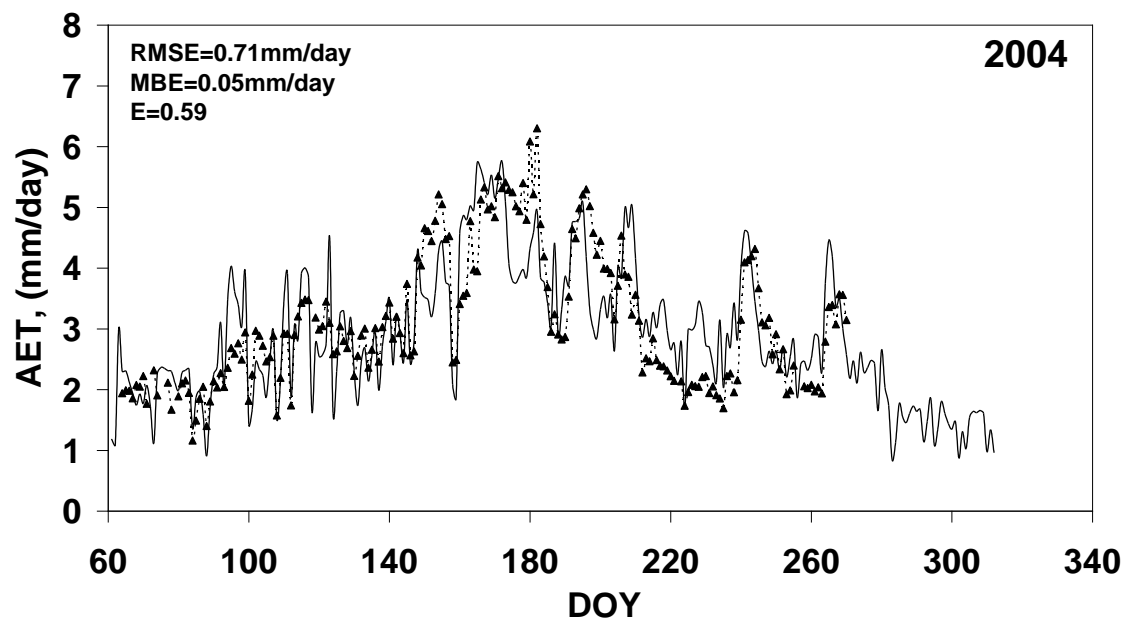


815
816
817

Figure 4



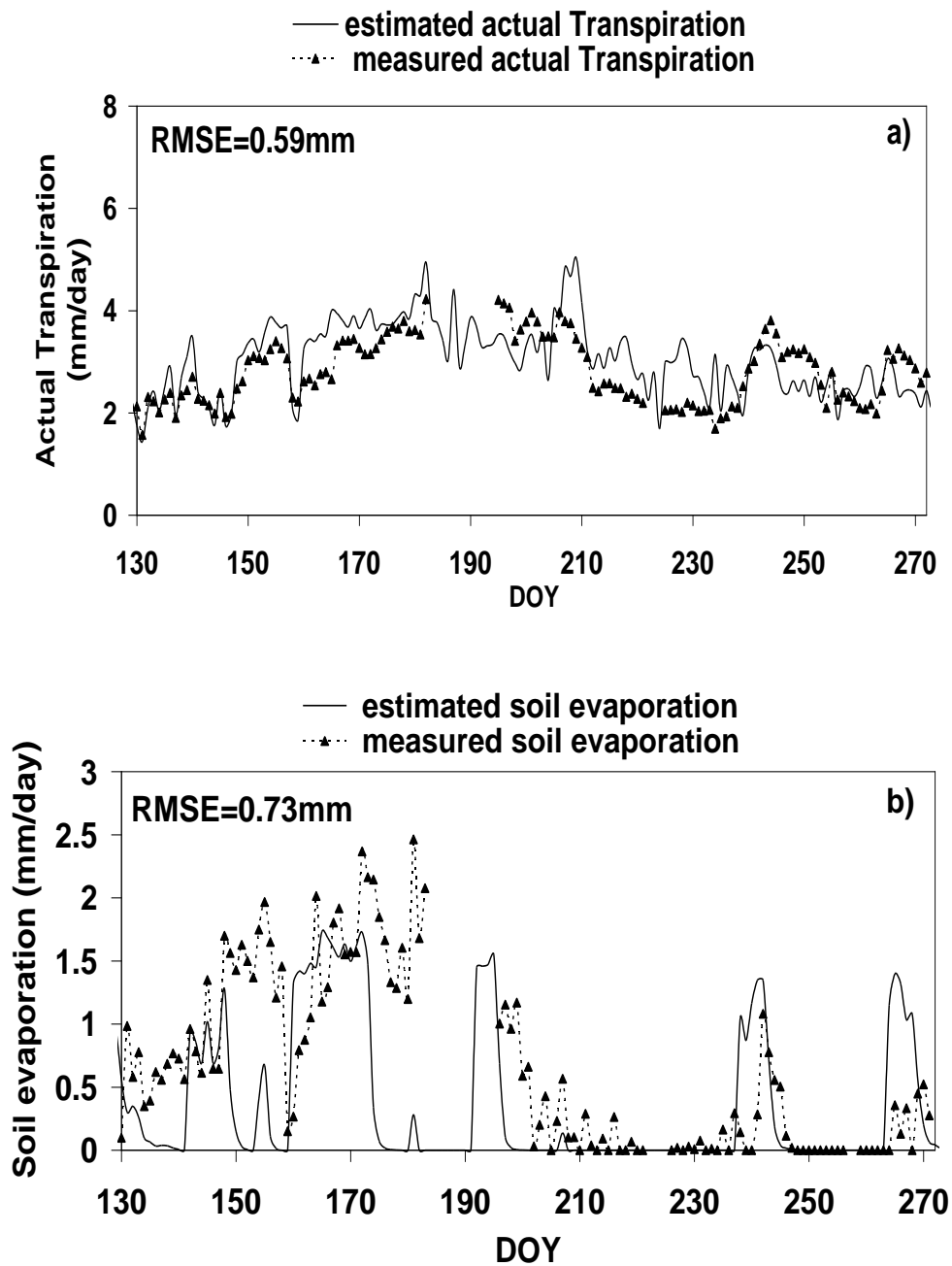
818



819
820
821

822
823
824

Figure 5



825

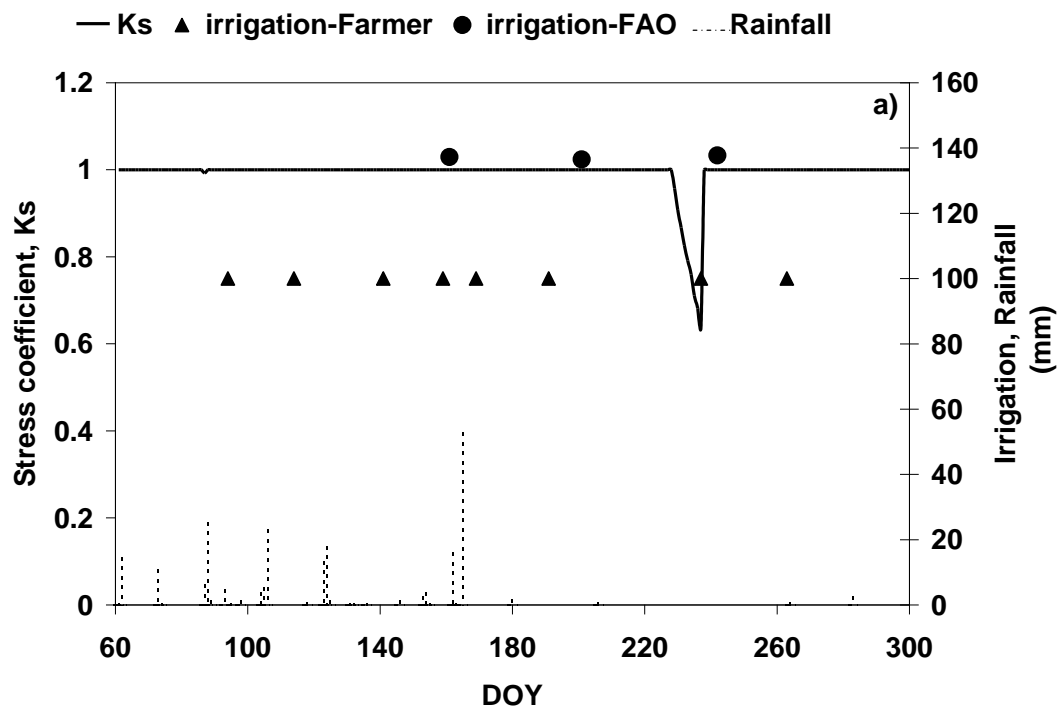
826

827

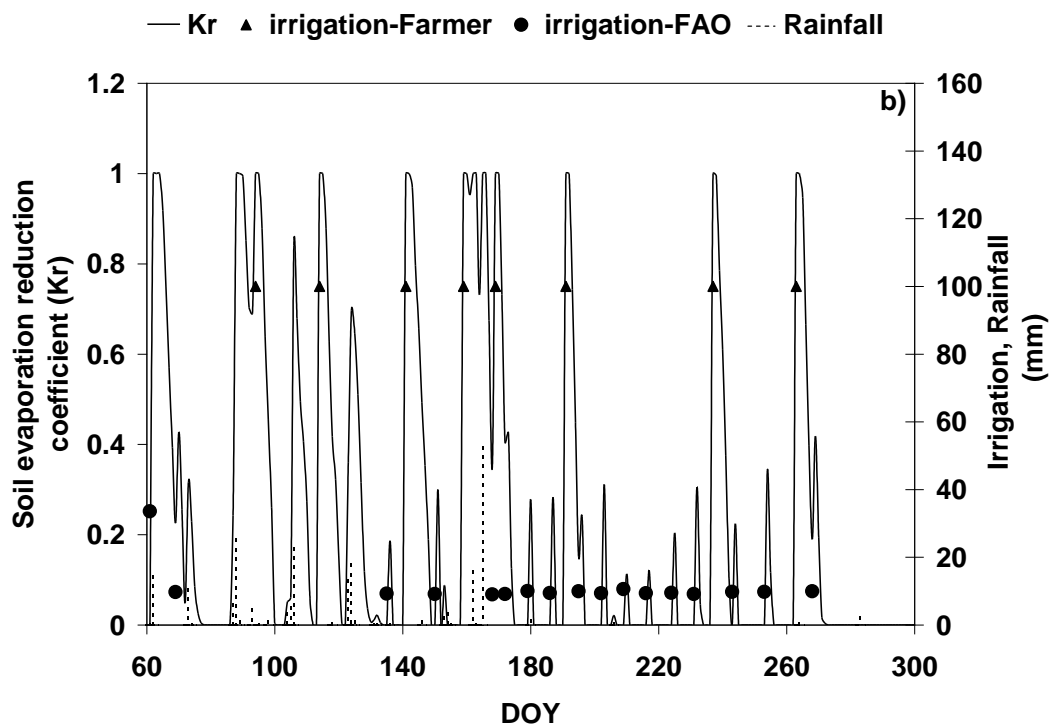
828

829
830
831

Figure 6



832
833
834



835
836
837
838
839